



**HAL**  
open science

# Non-Linear Partial-Least-Squares-based Polynomial Chaos Expansion (NLPLS-based PCE) approach for global sensitivity analysis of a High-Q Partially Air-Filled Pedestal Resonator Integrated in a Printed Circuit Board (PCB)

Leanne Johnson, Dieter Klink, Hassan Bouazzaoui, Elmine Meyer, Petrie Meyer, Benjamin Potelon, Cédric Quendo, Rozenn Allanic

## ► To cite this version:

Leanne Johnson, Dieter Klink, Hassan Bouazzaoui, Elmine Meyer, Petrie Meyer, et al.. Non-Linear Partial-Least-Squares-based Polynomial Chaos Expansion (NLPLS-based PCE) approach for global sensitivity analysis of a High-Q Partially Air-Filled Pedestal Resonator Integrated in a Printed Circuit Board (PCB). 56th CIRP International Conference on Manufacturing Systems 2023, Oct 2023, Cape Town, South Africa. pp.643-648, 10.1016/j.procir.2023.09.052 . hal-04449592

**HAL Id: hal-04449592**

**<https://hal.science/hal-04449592>**

Submitted on 9 Feb 2024

**HAL** is a multi-disciplinary open access archive for the deposit and dissemination of scientific research documents, whether they are published or not. The documents may come from teaching and research institutions in France or abroad, or from public or private research centers.

L'archive ouverte pluridisciplinaire **HAL**, est destinée au dépôt et à la diffusion de documents scientifiques de niveau recherche, publiés ou non, émanant des établissements d'enseignement et de recherche français ou étrangers, des laboratoires publics ou privés.

56th CIRP Conference on Manufacturing Systems, CIRP CMS '23, South Africa

## Non-Linear Partial-Least-Squares-based Polynomial Chaos Expansion (NLPLS-based PCE) approach for global sensitivity analysis of a High-Q Partially Air-Filled Pedestal Resonator Integrated in a Printed Circuit Board (PCB)

Leanne Johnson<sup>1\*</sup>, Dieter Klink<sup>1</sup>, Hassan Bouazzaoui<sup>2,3</sup>, Elmine Meyer<sup>4</sup>, Petrie Meyer<sup>1</sup>, Benjamin Potelon<sup>2,5</sup>, Cédric Quendo<sup>2</sup>, Rozenn Allanic<sup>2</sup>

<sup>1</sup>Electrical and Electronic Department, Stellenbosch University, Stellenbosch 7602, South Africa

<sup>2</sup>Laboratory-STICC, UMR CNRS 6285, CNRS, University of Brest, 29238 Brest, France

<sup>3</sup>Protecno Groupe Traon Industrie Développement, 29200 Brest, France

<sup>4</sup>Department of Electrical Engineering, Eindhoven University of Technology, 5612 AP Eindhoven, The Netherlands

<sup>5</sup>Laboratory-STICC, UMR CNRS 6285, IMT Atlantique, 29238 Brest, France

\* Corresponding author. E-mail address: [ljohnson@sun.ac.za](mailto:ljohnson@sun.ac.za).

### Abstract

This paper presents a global sensitivity analysis of a high-Q partially air-filled pedestal resonator integrated in a printed circuit board. Non-linear partial-least-squares-based polynomial chaos expansion (NLPLS-based PCE) approach is used for the global sensitivity analysis. Using NLPLS-based PCE a surrogate model is constructed with a reduced dimensionality, which enhances the performance of the algorithm. A standard PCE surrogate model, with all the system parameters, is created from the reduced NLPLS-based PCE surrogate model. The statistical information needed to perform the sensitivity analysis, i.e., variance, is extracted from the standard PCE surrogate model. A variance-based global sensitivity analysis is performed on the PCE model, each system parameter's sensitivity is quantified as the partial influence on the total variance of the performance variable S11. The chosen manufacturing technology involves a three-stage process: micromachining of the cavity, metallization, and thermos-diffusion stacking. During the three stages several problems may occur that can have an influence on the performance of the resonator, such as shape and size variation, and misalignment. The system parameters are set up according to these most common problems. The results show that, of the 8 system parameters chosen to evaluate, the height of the cavity and pedestal are the most sensitive parameters.

© 2023 The Authors. Published by Elsevier B.V.

This is an open access article under the CC BY-NC-ND license (<https://creativecommons.org/licenses/by-nc-nd/4.0>)

Peer-review under responsibility of the scientific committee of the 56th CIRP International Conference on Manufacturing Systems 2023

**Keywords:** Variance-based global sensitivity analysis; nonlinear partial-least-squares; polynomial chaos expansions; AFSIW; PCB process.

### 1. Introduction

Microwave filters are widely used in wireless communication systems, radar systems, test and measurement equipment, and global positioning systems (GPS). The design and manufacturing of microwave filters are complex tasks, requiring the optimization of multiple parameters. The need for

smaller, cheaper filters with low losses pose a challenge to microwave engineers and have led to the development of new manufacturing and design techniques to accomplish this goal. Waveguide resonators provides low loss and high Q resonators, however they are bigger and bulkier designs [1]. Planar resonators like microstrip or stripline are smaller and easier to integrate into systems but suffer from high losses due to the

dielectric material used [2]. A promising compromise to these drawbacks is Substrate integrated waveguide (SIW) resonators. SIW resonators are smaller than waveguide resonators and have lower losses and higher Q factors than microstrip or stripline resonators [3]. A popular approach to minimizing the footprint of microwave filters is to load the resonators. This has been applied successfully in SIW structures and is often accomplished with slots [4] or metal vias [5]. However, when applied to planar resonators the losses due to the substrate material are still present. A solution to this problem is to remove the substrate material partially or completely. However, previously this type of resonator was not manufacturable due to the need of supporting material for the loading structure. In 2022 a novel high-Q partially air-filled pedestal resonator was proposed as a solution [6]. This resonator was manufactured using a novel technological process based on micromachining and thermo-diffusion.

In recent years many new approaches to manufacturing microwave components have been investigated. In [7] an overview is given development of novel components and manufacturing technologies. In this paper the use of novel materials such as paper and textile are introduced and applied to SIW structures with the use of 3D printing and additive manufacturing. There have been two approaches showcased for producing SIW components on paper: one utilizes ink-jet printing [8], while the other employs the milling technique [9]. Another popular manufacturing technique is 3D-printing. In [10] the use of 3D-printed alumina ceramics to achieve variable dielectric constants for novel microwave applications is investigated. However, there are still gaps in knowledge on the effect and possibilities of these novel manufacturing techniques.

Global sensitivity analysis (GSA) and yield estimation are powerful tools that are used to identify important parameters and their interactions in a design. GSA and yield estimation provides valuable information on the behavior of a system and minimizes the need for multiple redesigns and therefore lowers cost.

Manufacturing tolerances refer to the permissible variations in the dimensions and other characteristics of a manufactured product. Manufacturing tolerances may lead to faulty components or systems. Therefore, it is important to estimate the yield and sensitivity, considering manufacturing tolerances, when microwave systems are designed. This is especially true when new manufacturing techniques are used, to ensure the processes and techniques are suitable for large scale production.

Studies on sensitivity analysis applied to microwave systems have used various variance based methods including Standard Monte Carlo methods [11], finite-difference time- and frequency domain methods [12,13], stochastic collocation methods [14], and Polynomial Chaos Expansion (PCE) methods [15]. These aforementioned studies show that identifying critical parameters and their influence in the system is possible. However, when used on their own, many of the methods in [11,12,13,14] are not suitable for problems with high dimensionality and non-linearity of the system, which becomes computationally too expensive. Recent studies have

focused on developing new methods for global sensitivity analysis that can handle high-dimensional and nonlinear systems [16]. These studies utilize chaos expansion and neural networks [15,17], showing accurate results that can handle high dimensionality and nonlinearity of the system.

In this paper Non-Linear Partial Least Squares - based PCE (NLPLS-based PCE) is used for a sensitivity analysis on the newly proposed partially air-filled pedestal SIW resonator in [6]. The pedestal SIW resonator has progressed from an initial filled cavity structure [18], to implementation in a partially air-filled SIW [6]. This was done to increase the Q factor of the resonator. The manufacturing technology involved in the creation of the partially AFSIW involved three stages: micromachining of the cavity, metallization and thermo-diffusion stacking. Problems such as alignment, conductive continuity, and warping may arise with this manufacturing techniques. To determine the reliability a repeatability of the desired manufacturing technique, a sensitivity analysis is performed and presented in this paper.

## 2. NLPLS-based PCE

As presented in [19], PLS-based PCE is the combination of PCE and Partial Least Squares (PLS). PCE is used to construct a stochastic model consisting of a polynomial expansion representing the electromagnetic model. NLPLS is the adaptation of PLS to non-linear systems.

### 2.1. Non-linear partial least squares

As detailed in [20], PLS aims to identify linear transformations of the system parameters that are highly related to the performance parameter of interest, while being independent of one another. PLS assumes that the system parameters are linearly related to the performance variable. If this assumption is not met, if the underlying structure of the system exhibits non-linear characteristics, then a Non-Linear PLS (NLPLS) approach would be used instead, as proposed by [21]. NLPLS is used to reduce the dimensionality of the problem with the use of latent variables.

A data matrix, represented as  $X$ , is composed of a set of  $N$  samples obtained from a random variable vector, denoted as  $x = \{x_1, x_2, \dots, x_n\}$ . A vector of performance outcomes,  $Y$ , is established based on the evaluations of the electromagnetic simulations done in CST Studio Suite on the data matrix  $X$ . In accordance with standard procedures, PLS projects the data matrix  $X$  onto the latent components ( $t_i$ ) by successively maximizing the covariance between  $Y$  and  $t_i$ , where  $t_i = \{t_{1i}, t_{2i}, \dots, t_{ni}\}$ . To account for the non-linearity of the system, the nonlinear correlation between  $Y$  and  $t_i$  is modeled as a polynomial function, where Ordinary Least Squares (OLS) is used to calculate the coefficients. A comprehensive mathematical explanation can be found in and [19] and [21].

2.2. Polynomial chaos expansion

PCE takes advantage of the orthogonality of polynomials when using different functions to distribute the parameters. PCE is particularly well-suited for handling uncertainty or randomness in the design process and is therefore a better choice than other polynomial-based methods [14,23]. The  $Y(x)$  performance variable is modeled using equation (1):

$$Y(x) = \sum_{k=0}^{\infty} c_k \psi_k(x) \tag{1}$$

The set  $k = \{k_1, k_2, \dots, k_n\}$  represents the  $k^{th}$  component to the  $n^{th}$  degree,  $c_k$  represents the polynomial coefficients, and  $\Psi_k(x)$  represents the multivariate Hermite polynomials. A detailed explanation on PCE can be found in [16]. The multivariate Hermite polynomials are constructed with a set of statistically independent variables as follows:

$$\Psi_k(x) = \prod_{i=1}^n \psi_{k_i}(x_i) \tag{2}$$

The univariate Hermite polynomials for each system parameter  $x_i$  are represented by  $\psi_{ki}$ , where  $k = \{k_1, k_2, \dots, k_n\}$ . The PCE is truncated to only include  $P$  terms as follows:

$$Y(x) = \sum_{|k| \leq p}^P c_k \psi_k(x) \tag{3}$$

Assuming the PCE is a sufficiently accurate approximation, the mean and variance can be obtained by using equations (4) and (5) respectively.

$$\mathbb{E}\{y(x)\} \approx c_0 \alpha_0 \tag{4}$$

$$Var\{y(x)\} \approx \sum_{|k| \leq p}^P c_k^2 \alpha_k^2 \tag{5}$$

Where,

$$\alpha_k^2 = \langle \psi_k(x), \psi_k(x) \rangle = \int \psi_k w(x) dx \tag{6}$$

The joint PDF of the random system parameter vector  $x$  is represented by  $w(x)$  and the support of the random system parameter vector is represented by  $\Gamma$ . In NLPLS, PCE is used as a non-linear polynomial function that connects the latent component  $t_i$  with the response vector  $Y$ , resulting in a one-dimensional expansion of degree  $p$  using Hermite polynomials.

$$\hat{Y}_i^p(t) = \sum_{i=1}^P \hat{c}_{ij}^p \psi_j(t_i) \tag{7}$$

The PCE regression for the initial latent variable can be described as:

$$y = \sum_i^p c_{1j}^p \psi_j(t_1) + e \tag{8}$$

As stated in [22] the PDF of the transformed basis  $t_1$  remains orthogonal to the Hermite polynomial base. Each latent component is evaluated with different polynomial degrees  $q = \{1, \dots, p\}$  the degree that has the minimal leave-one-out error  $\epsilon q$  LOO is then selected as the appropriate polynomial degree for that specific latent variable [23]. The fitting error vector  $F$  is then minimized by using the PCE described and the NLPLS method outlined in [16] until a predefined error threshold is met. Subsequently, a set of  $m$  latent components,  $m$  weights, and  $m$  PCE models are obtained. The final version of the metamodel, is then created.

$$\hat{Y}_m^{PLS}(x) = b_0 + \sum_{i=1}^m \hat{Y}_i^{qi} \left[ (r_i^{qi})^T \tilde{x} \right] \tag{9}$$

The value  $q_i$  represents the degree of the  $i^{th}$  principal component of the PCE metamodel, with the lowest leave-one-out cross-validation error ( $\epsilon$ LOO). The matrix  $R$  is used to express the set of target values 'T' as a projection of the data matrix  $X$  onto the matrix  $R$ . This metamodel is verified through the comparison of its predictions with the actual results obtained from the model evaluations, with the use of the Root Mean Square Error (RMSE) as the measure of accuracy.

$$RMSE = \sqrt{\sum_{i=1}^N (\hat{Y}_i - Y_i)^2 / N} \tag{10}$$

Once the metamodel is found to have a high level of accuracy, as demonstrated by a small Root Mean Square Error, statistical information can be derived directly from the linear PCE's coefficients. This includes the sum of variance and mean estimates for each latent component.

$$\hat{\sigma}_{Y_m^{PLS}} = \sum_i^m \sigma_{\hat{Y}_i^{qi}} \tag{11}$$

$$\hat{\mu}_{Y_m^{PLS}} = \sum_i^m \mu_{\hat{Y}_i^{qi}} \tag{12}$$

2.3. Global sensitivity analysis

The assessment of overall sensitivity, known as global sensitivity analysis, is performed as a subsequent step after a NLPLS-based PCE surrogate model with an acceptable level of accuracy is established. The surrogate model is firstly transformed back into a standard PCE, consisting of all the system parameters. Then the effect of each system parameter is calculated and compared with the overall variance of the

performance parameter. Research in [24] has shown that the NLPLS-based PCE surrogate,  $\hat{Y}_m^{PLS}$ , can be used to assess the sensitivity to the original system parameter vector  $x$ . The following equation is used to convert the NLPLS-based PCE coefficients  $b$  to standard the PCE coefficients  $c$ :

$$c_k = \sum_{i=1}^m b_{i|k}^{q_i} \sqrt{|k|!} \prod_{i=1}^d \frac{r_{it}^{k_i}}{\sqrt{k_i!}} \quad (13)$$

The  $il^{th}$  entry in matrix  $R$  is represented by  $r_{il}$ , where  $m$  represents the number of latent components,  $k$  represents the multi-index, and  $b$  represents the NLPLS-based PCE coefficients. The NLPLS-based PCE can be expressed in the traditional way with these coefficients.

$$\hat{Y}_m^{PLS} = c_0 + \sum_{|k| \leq q_{max}} c_k \psi_k(x) \quad (14)$$

$$q_{max} = \operatorname{argmax}(q_i) \quad i \in \{1, \dots, m\} \quad (15)$$

The authors in [16] demonstrates that the mean and variance can easily be obtained from a truncated PCE with  $P$  terms, as given by (3), using (4) and (5) respectively. Additionally, [25] has shown that the Sobol' indices for (3) can be calculated through post-processing the coefficients  $c$ . The final PCE-based sensitivity indices, as outlined in [24], are:

$$\hat{S}_{\hat{Y}, A}^T = \frac{1}{\sqrt{\hat{Y}}} \sum_{j^k \neq 0} c_k^2 \quad (16)$$

Boolean index vector  $I^A$  is used for a specific subset of input variables, denoted by the index  $A$ , where  $I^{Ai} = 0$  if  $i$  is not in  $A$  and  $I^{Ai} = 1$  if  $i$  is in  $A$ . Similarly, we use a Boolean vector for the multi-index  $k$ , where  $I^{ki} = 0$  if  $k_i = 0$  and  $I^{ki} = 1$  if  $k_i > 0$ .

### 3. Partially air-filled pedestal resonator

The original pedestal resonator is a type of loaded cavity, typically made of a classical SIW material, that contains a metal plate at an intermediate height and one or more metal posts on one side, creating a short-circuit. In order to decrease losses and enhance Q-factors of SIW structures the dielectric material can be removed. An alternative called air-filled SIW (AFSIW) was implemented to create the partially air-filled pedestal resonator seen in Fig. 1. This resonator is designed to operate at 5 GHz.

Traditionally, Air-Filled- or Empty- Substrate Integrated Waveguides on Printed Circuit Boards (PCB) are made by milling a double-sided board and attaching copper foils with bolts. However, for this structure a manufacturing techniques that allows for the support of the pedestal is needed. To overcome this issue, a three-stage manufacturing method is selected which involves: micromachining of the cavity, metallization, and thermo-diffusion stacking. This process

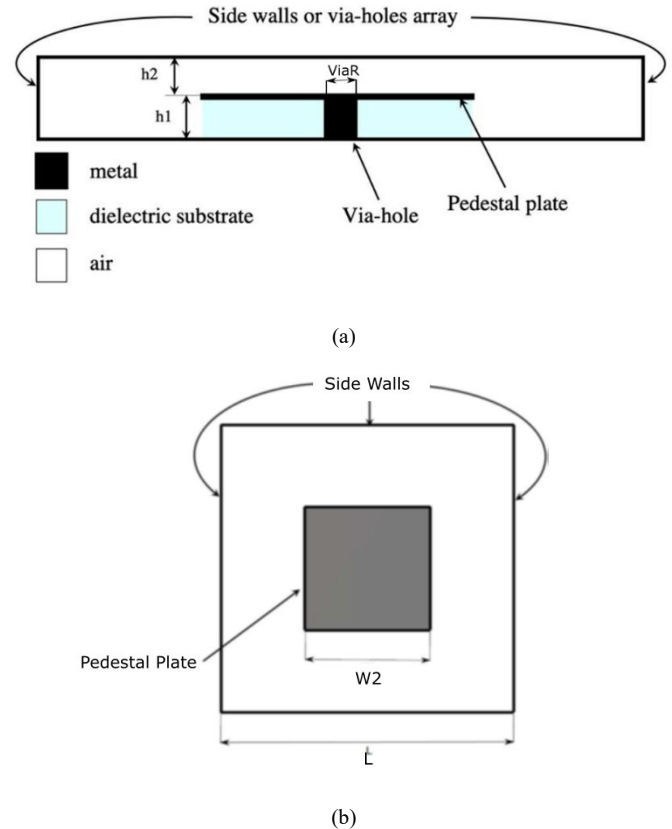


Figure 1: (a) Side view of partially air-filled pedestal resonator and (b) Top view of partially air-filled pedestal resonator [6].

allows for a solid assembly while eliminating the need for any additional mechanical structural support (screws, etc.) The process is described in detail in [18]. This application poses a computationally expensive task, with 8 sensitive system parameters ( $x = \{h_1, h_2, W2, W1, L, ViaR, InputW, InputL\}$ ), making it a perfect example to demonstrate the benefits of using NLPLS-based PCE. The step-by-step manufacturing process is as follows (the dielectric substrate is represented in blue, the air in white, and the metallization in black):

- The pedestal shape is created with a depth-controlled micro-machining or laser-based technique on a classical copper-cladded double-side dielectric board (as seen in Fig. 3(a)). This process selectively removes parts of the substrate and metal, resulting in the structure shown in Fig. 3(b).
- Via-holes are drilled as seen in Fig. 3(c).
- Metallization of all surfaces, including the via-holes, cavity sidewalls, and pedestal edges, as depicted in Fig. 3(d).
- De-metallized of specific areas such as the pedestal or access edges with a precision milling machine or laser as shown in Fig. 3(e).
- A 35-micrometer-thick copper foil is bonded onto the top of the structure via thermo-diffusion to create an enclosed quasi-empty SIW cavity, as shown in Fig. 3 (f).

The final manufacturable design can be seen in Fig. 2.

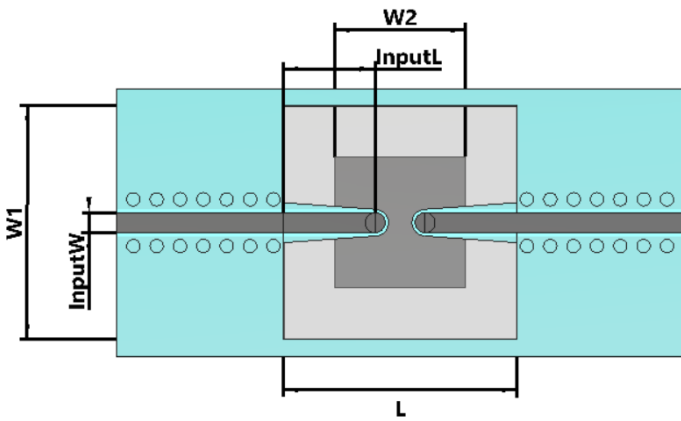


Figure 2: Top view of manufacturable resonator.

#### 4. Results

The variables that are of interest for this study are the following:  $x = \{h_1, h_2, W2, W1, L, ViaR, InputW, InputL\}$ . A study is conducted in which a Gaussian variation with mean of 0 mm and variance of 1  $\mu\text{m}$  ( $N(0,001)$ ) is applied to each variable of the optimal design  $x_0$ . For this design  $S_{11}$  is used as the performance parameter at 5 GHz. The resonator designed in [9] was designed to operate at 5GHz with a bandwidth of 5%. The criteria to be met is -17 dB between a 5% bandwidth. The NLPLS-based PCE estimate closely approximates the true PDF with only 30 samples, which suggests a precise portrayal of the true statistical data.

The sensitivity analysis, which is processed post-simulation, at the center frequency of 5 GHz can be seen in Fig. 4. The statistically significant system parameters are  $x = \{h_1, h_2, W2, W1, L, ViaR, InputW, InputL\}$ . The nominal design consists of  $x_0 = \{0.5, 0.5, 7.84, 14, 14, 0.4, 5.5\}$ . The results show that the resonator is most sensitive to changes in  $h_1$  and  $h_2$ . This result shows that during manufacturing the most care must be taken to ensure the micro-machining is done to the correct height and during the thermo-diffusion stage that the metal being used as the top and bottom metal layer to enclose the cavity is able to withstand the needed temperature and pressure to avoid any warping that may occur. Care must also be taken that the height of the pedestal and copper thickness of the plate is accurate enough for constant height ( $h_2$ ) above the pedestal. For the pedestal resonator the electric field is concentrated above the pedestal patch while the magnetic field is concentrated around the pedestal post. The result from the sensitivity analysis shows that there is a greater dependence on the overall response on the electric field change than that of the magnetic field change. Laser cutting is generally considered to be more precise than micro machining when it comes to cutting away material. Therefore, it would be beneficial to use this method instead of micro machining the material away.

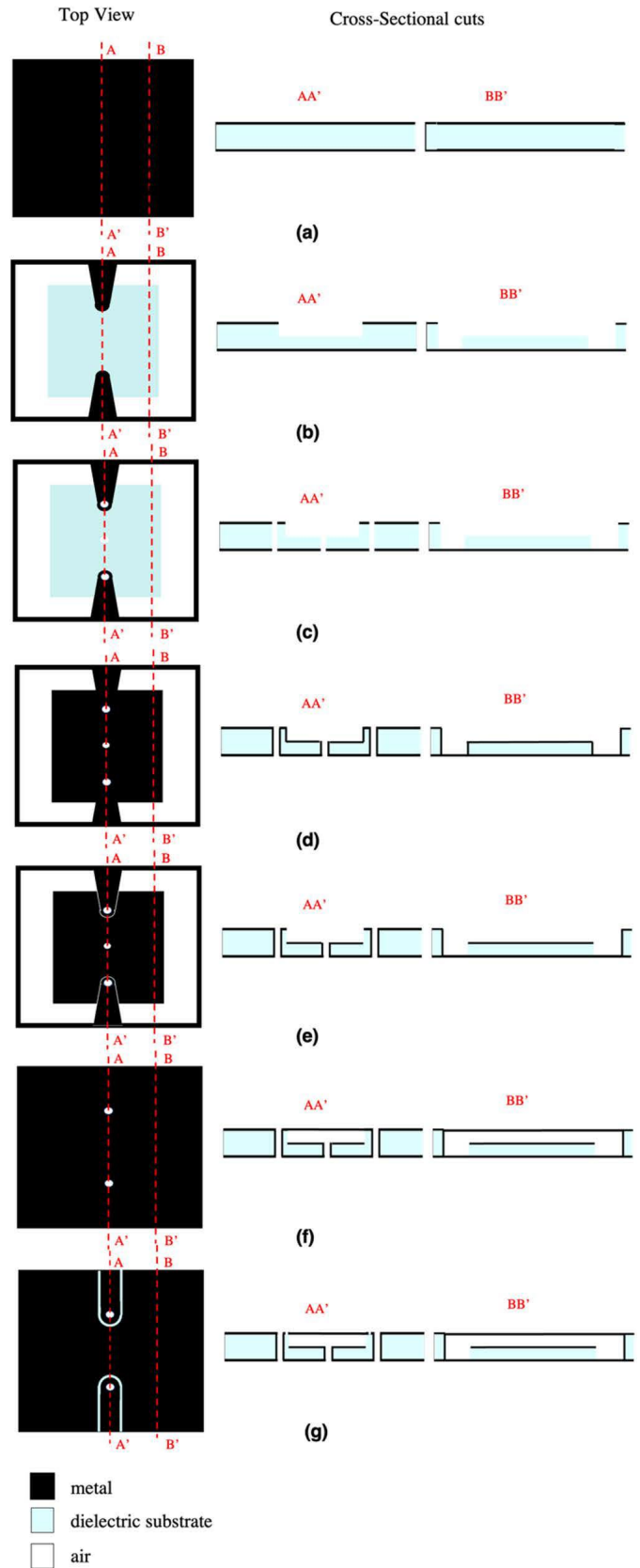


Figure 3: Steps of the technological process. (a) initial double-side copper-clad substrate, (b) micro-machining, (c) via-hole drilling, (d) metallizing, (e) selective de-metallizing, (f) cavity closing, (g) feeding lines etching [9].



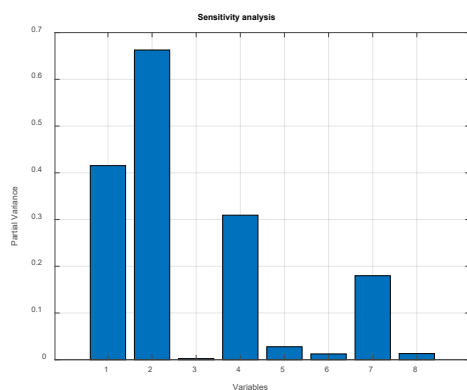


Figure 4: Sensitivity analysis of partially air-filled SIW resonator

## 5. Conclusion

This study conducts a comprehensive sensitivity analysis on a high-Q partially air-filled pedestal resonator that is integrated in a printed circuit board in order to determine the manufacturing repeatability and reliability. The analysis utilizes a NLPLS-based PCE approach. A variance-based global sensitivity analysis is performed on the surrogate model, and each system parameter's sensitivity is quantified as the partial influence on the total variance of the performance variable S11. The chosen manufacturing technology involves a three stages process: micromachining of the cavity, metallization, and thermos-diffusion stacking. The results indicate that among the 8 system parameters evaluated, the height of the cavity and pedestal are the most sensitive parameters. It is suggested to make use of laser cutting instead of micro-machining to cut the pedestal shape to make repeatable and reliable production more likely. To stack the top and bottom plates on the top and on the bottom to seal the cavity, it is suggested to use a stronger metal that will reduce the chances of bending and altering the total height of the cavity during the thermo-diffusion process. Other solutions to allow for an air filled cavity with a pedestal load could be to use 3D printing techniques. It is also suggested to look into Low-Temperature Co-fired Ceramic Technology (LTCC) to design a resonator with a material with lower losses such as ceramics or techniques using paper [7].

## References

- [1] Q. Huang and Z. Wu, "A compact six-order folded-waveguide resonator filter," 2018 IEEE MTT-S International Wireless Symposium (IWS), Chengdu, China, 2018, pp. 1-4, doi: 10.1109/IEEE-IWS.2018.8400906.
- [2] A. Munir, R. Safitri and M. R. Effendi, "Development of microstrip BPF using open split ring resonator with square groundplane window," 2014 International Symposium on Antennas and Propagation Conference Proceedings, Kaohsiung, Taiwan, 2014, pp. 49-50, doi: 10.1109/ISANP.2014.7026524.
- [3] Y. D. Parmar and S. C. Bera, "Investigation of substrate integrated waveguide filters and construction technique," 2017 International Conference on Computing Methodologies and Communication (ICCMC), Erode, India, 2017, pp. 738-740, doi: 10.1109/ICCMC.2017.8282564.
- [4] S. K. Thapa, B. Chen, A. Barakat, K. Yoshitomi and R. K. Pokharel, "Miniaturized Slot-Loaded SIW Resonator and Its Application to C-band Low Phase Noise Oscillator," 2020 50th European Microwave Conference (EuMC), Utrecht, Netherlands, 2021, pp. 161-164, doi: 10.23919/EuMC48046.2021.9338129.
- [5] M.-H. Ho, J.-C. Li and Y.-C. Chen, "Miniaturized SIW Cavity Resonator and Its Application in Filter Design," in IEEE Microwave and Wireless Components Letters, vol. 28, no. 8, pp. 651-653, Aug. 2018, doi: 10.1109/LMWC.2018.2845101.
- [6] L. Johnson et al., "Novel High-Q Partially Air-Filled Pedestal Resonator and Filter Integrated in a Printed Circuit Board (PCB)," IEEE Access, vol. 10, no. September, pp. 101160-101167, 2022, doi: 10.1109/ACCESS.2022.3208351.
- [7] S. Moscato, L. Silvestri, N. Delmonte, M. Pasian, M. Bozzi and L. Perregrini, "SIW components for the Internet of Things: Novel topologies, materials, and manufacturing techniques," 2016 IEEE Topical Conference on Wireless Sensors and Sensor Networks (WiSNet), Austin, TX, USA, 2016, pp. 78-80, doi: 10.1109/WISNET.2016.7444327.
- [8] S. Kim, B. Cook, T. Le, J. Cooper, H. Lee, V. Lakafosis, R. Vyas, R. Moro, M. Bozzi, A. Georgiadis, A. Collado, M. Tentzeris, "Inkjet-printed Antennas, Sensors and Circuits on Paper Substrate," IET Microwaves, Antennas and Propagation, Vol. 7, No. 10, pp. 858-868, July 16, 2013.
- [9] S. Moscato, N. Delmonte, L. Silvestri, M. Pasian, M. Bozzi, and L. Perregrini, "Compact Substrate Integrated Waveguide (SIW) Components on Paper Substrate," 45th European Microwave Conference (EuMC2015), Paris, France, Sept. 7-10, 2015.
- [10] L. Robins, A. Arsanjani, C. Bartlett, R. Teschl, W. Bösch and M. Höft, "Additive Manufacturing of Non-homogenous Dielectric Waveguide Structures and Filters," 2021 IEEE MTT-S International Microwave Filter Workshop (IMFW), Perugia, Italy, 2021, pp. 326-328, doi: 10.1109/IMFW49589.2021.9642291.
- [11] Sadiku, M.N.O. (2009). Monte Carlo Methods for Electromagnetics (1st ed.). CRC Press. <https://doi.org/10.1201/9781315218465>
- [12] S. M. Smith and C. Furse, "Stochastic FDTD for analysis of statistical variation in electromagnetic fields," IEEE Trans. Antennas Propag., vol. 60, no. 7, pp. 3343-3350, 2012, doi: 10.1109/TAP.2012.2196962.
- [13] K. Masumnia-Bisheh, K. Foroogari, and M. Ghaffari-Miab, "Electromagnetic Uncertainty Analysis Using Stochastic FDFD Method," IEEE Trans. Antennas Propag., vol. 67, no. 5, pp. 3268-3277, 2019, doi: 10.1109/TAP.2019.2896771.
- [14] J. Bai, G. Zhang, L. Wang, and T. Wang, "Uncertainty analysis in EMC simulation based on improved method of moments," Appl. Comput. Electromagn. Soc. J., vol. 31, no. 1, pp. 66-71, 2016.
- [15] P. Manfredi, D. Vande Ginste, D. De Zutter, and F. G. Canavero, "Generalized Decoupled Polynomial Chaos for Nonlinear Circuits with Many Random Parameters," IEEE Microw. Wirel. Components Lett., vol. 25, no. 8, pp. 505-507, 2015, doi: 10.1109/LMWC.2015.2440779.
- [16] D. Klink, P. Meyer, and W. Steyn, "Efficient sensitivity analysis of EM structures using NLPLS-based PCE," 2022 Int. Conf. Electromagn. Adv. Appl. ICEAA 2022, vol. 14, no. 8, pp. 366-371, 2022, doi: 10.1109/ICEAA49419.2022.9900042.
- [17] S. A. Sadrossadat, Y. Cao, and Q. J. Zhang, "Parametric modeling of microwave passive components using sensitivity-analysis-based adjoint neural-network technique," IEEE Trans. Microw. Theory Tech., vol. 61, no. 5, pp. 1733-1747, 2013, doi: 10.1109/TMTT.2013.2253793.
- [18] S. O. Nassar and P. Meyer, "Pedestal substrate integrated waveguide resonators and filters," IET Microwaves, Antennas Propag., vol. 11, no. 6, pp. 804-810, 2017, doi: 10.1049/iet-map.2016.0120.
- [19] I. Papaioannou, M. Ehre, and D. Straub, "PLS-based adaptation for efficient PCE representation in high dimensions," J. Comput. Phys., vol. 387, pp. 186-204, 2019, doi: 10.1016/j.jcp.2019.02.046.
- [20] A. Höskuldsson, "PLS regression methods," J. Chemom., vol. 2, no. 3.
- [21] G. Baffi, E. B. Martin, and A. J. Morris, "Non-linear projection to latent structures revisited: The quadratic PLS algorithm," Comput. Chem. Eng., vol. 23, no. 3, pp. 395-411, 1999, doi: 10.1016/S0098-1354(98)00283-X.
- [22] R. Tipireddy and R. Ghanem, "Basis adaptation in homogeneous chaos spaces," J. Comput. Phys., vol. 259, pp. 304-317, 2014, doi: 10.1016/j.jcp.2013.12.009.
- [23] B. To and H. A. L. Id, "Chaos polynomial creux et adaptatif pour la propagation d'incertitudes et l'analyse de sensibilité géométrique BLATMAN Docteur d'Université," 2009.
- [24] M. Ehre, I. Papaioannou, and D. Straub, "Global sensitivity analysis in high dimensions with PLS-PCE," Reliab. Eng. Syst. Saf., vol. 198, no. November 2019, p. 106861, 2020, doi: 10.1016/j.res.2020.106861.
- [25] B. S. Å, "Global sensitivity analysis using polynomial chaos expansions," vol. 93, pp. 964-979, 2008, doi: 10.1016/j.res.2007.04.002.